—Original—

Chronic Ablation Lesions after Cryoballoon and Hot Balloon Ablation of Atrial Fibrillation

Ryuta Watanabe, Yasuo Okumura, Koichi Nagashima,
Yuji Wakamatsu, Akimasa Yamada and Sayaka Kurokawa

Division of Cardiology, Department of Medicine, Nihon University School of Medicine, Tokyo, Japan

Background: Chronological changes in ablation lesions after cryoballoon ablation (CBA) and hot balloon ablation (HBA) of atrial fibrillation (AF) remain unclear.

Methods: Of 90 patients who underwent initial balloon-based catheter ablation of AF and cardiac magnetic resonance imaging (cMRI) 3 months after ablation, data from 48 propensity score-matched patients (24 per group; 34 males; age 62±10 years) were analyzed. High-density pulmonary vein-left antrum (PV-LA) voltage mapping was performed after PV isolation, and low voltage areas around the PV ostia were defined as the total acute ablation lesion area (cm^2). cMRI-derived dense fibrotic tissue localized around PVs was defined as the total chronic ablation lesion area (cm^2). The percentage of total ablation lesion areas to total PV-LA surface area (%ablation lesion) was calculated during each phase, and %acute ablation lesion and %chronic ablation lesion areas were compared in patients who had undergone CBA and HBA.

Results: The %acute ablation lesion area was larger for the CBA group than for the HBA group (30.8±5.8% vs. 23.0±5.5%, $p < 0.001$). There was no difference in %chronic cMRI-derived ablation lesion area (24.8±10.8% vs. 21.1±11.6%, $p = 0.26$) between groups. The rates of chronic AF recurrence were 12.5% and 8.3%, respectively ($p = 0.45$; log-rank test). LA volume and LA surface area were strongly associated with AF recurrence, but %chronic ablation lesion area was not (27±8% vs. 23±12%, $p = 0.39$).

Conclusion: Large acute ablation lesions after CBA were smaller during the chronic phase. The size of chronic ablation lesions and the rate of AF recurrence were both similar for CBA and HBA.

(J Nippon Med Sch 2023; 90: 69–78)

Key words: atrial fibrillation, cyroballoon, hot balloon, magnetic resonance image

Introduction

Balloon technologies have been developed to simplify pulmonary vein isolation (PVI) in atrial fibrillation (AF). Cryoballoon ablation (CBA) was approved in Japan in 2014 and hot balloon ablation (HBA) in 2015. CBA is successful for 78-84% of cases and HBA for 59-84% of cases[1–6]. The efficacy of these balloon ablation technologies appears similar to that of standard radiofrequency (RF) contact force-guided PVI for patients with paroxysmal AF[7,8].

Although the success rates of balloon- and RF-based PVI procedures over 1 year are similar, acute PV ablation lesions on voltage maps were reported to be slightly larger, and the prevalence of acute PV gaps lower, after CBA than after HBA or RF ablation[4,6,9,10]. Nonetheless, several studies reported that PV gaps on voltage maps are evident chronically despite wide and persistent PV lesions in the acute phase after CBA[11,12]. This raises a question as to whether voltage map assessment of acute ablation lesions accurately reflects chronic ablation lesions. Gadolinium-enhanced cardiac magnetic resonance imaging (cMRI) can identify PV ablation lesions created by several energy sources, including RF, laser, and CB-based PVI during the chronic phase[13–15]. No studies have exam-

Correspondence to Yasuo Okumura, MD, PhD, Division of Cardiology, Department of Medicine, Nihon University School of Medicine, 30–1 Ohyaguchi-kamicho, Itabashi-ku, Tokyo 173–8610, Japan
E-mail: okumura.yasuo@nihon-u.ac.jp
https://doi.org/10.1272/jnms.JNMS.2023_90-112
Journal Website (https://www.nms.ac.jp/sh/jnms/)

ined chronological changes in ablation lesions after CBA and HBA and the impact of chronic cMRI-derived lesions on clinical outcomes. Therefore, we compared acute ablation lesions assessed by voltage maps and chronic ablation lesions assessed by cMRI after CBA and HBA and investigated whether chronic ablation lesions were associated with clinical outcomes.

Methods

Study Patients

We identified 90 patients who underwent initial catheter ablation of AF and cMRI 3 months after ablation between November 2016 and September 2018. Ten of the 90 patients were excluded from the analysis, however, because cMRI image quality was poor. Thus, 80 patients (45 patients for CBA and 35 for HBA) were included in the analysis. To accurately compare ablation lesions after CBA and HBA, we used propensity score matching to align patient background characteristics that affected late gadolinium enhancement of the left atrium (LA), such as AF subtype, age, hypertension, and structural heart disease, as described below[16–18]. A total of 48 propensity score-matched patients (24 patients per group; 34 males, 14 females; age 62±10 years) were included in this study. Anticoagulants were administered for at least 1 month before PVI, to ensure adequate oral anticoagulation, and all antiarrhythmic drugs (AADs) were discontinued for at least 5 half-lives before PVI. All patients provided informed consent for the use of their anonymized clinical data for research purposes, and our access to patient information was approved by the institutional review board of Nihon University Itabashi Hospital (November 13, 2015; RK-150908-8).

Electrophysiological Study and Acute PV Lesions Assessed by Voltage Mapping

All patients underwent an electrophysiological study under conscious sedation with dexmedetomidine, propofol, and fentanyl. After vascular access was obtained, a single transseptal puncture was performed, and intravenous heparin was administered to maintain an activated clotting time of >300 seconds. The 3-dimensional (3D) geometry of the LA and 4 PVs was reconstructed, and high-density PV-LA bipolar voltage mapping was performed during sinus rhythm (SR) with an Ensite NavX Velocity mapping system (Abbott, IL, USA) before and after PVI. The voltage map was created after PVI and touch-up ablation if patients had any acute PV reconnection sites. In patients with an AF rhythm, the voltage map was created after SR was restored by internal low-energy electrical cardioversion (15-20 joules). Bipolar signals, high-pass filtered at 30 Hz and low-pass filtered at 500 Hz, were acquired using a multipole, 20-pole, circular mapping catheter with a 4-mm interelectrode spacing (Inquiry AFocus II EB; Abbott). Areas with a peak-to-peak bipolar electrogram amplitude of <0.5 mV were defined as low-voltage areas. The PV ostium was identified as the point of maximal inflection between the PV wall and LA wall. The distal border of each PV was defined as the site adjacent to the major first bifurcation, and the 4 PVs distal to the distal border and LA appendage were subtracted first. The low voltage area around the PV ostium was measured on a voltage map after PVI: this area was defined as the total acute ablation lesion area (cm^2). This area was then subdivided into 4 PV lesions (left superior PV [LSPV], left inferior PV [LIPV], right superior PV [RSPV], and right inferior PV [RIPV]) by using the PV carina region lines. The %acute ablation lesion area was calculated as the total acute ablation lesion area (cm^2) (or acute ablation lesion in each PV)/ total PV-LA surface area (cm^2), which was determined by the total area of the LA body and 4 PV surfaces (**Fig. 1A, B**).

CBA and HBA

CBA was performed with a 28-mm CB (Arctic Front Advance; Medtronic, Minneapolis, USA) with an inner lumen mapping catheter (Achieve, Medtronic) placed in the LA through a 15 Fr deflectable sheath (Flexcath Advance, Medtronic) in standard fashion, as previously reported[9,10]. In brief, the balloon was then inflated and advanced successively to each PV ostium to establish optimal PV occlusion, as indicated by the absence of contrast leakage. Single-shot cryoenergy was delivered for 180 seconds to each PV after occlusion was established.

HBA was performed with an HB device (SATAKE Hotballoon; Toray Industries Inc, Tokyo, Japan) with an inner lumen and J-tip guidewire, as previously reported[4,6]. The J-tip guidewire was inserted into the target PV, and the HB was inflated to 26-33 mm at each PV ostium through a 13 Fr deflectable guiding sheath (Treswaltz; Toray Industries). After optimal PV occlusion was achieved by contrast injection, an RF current of 1.8 MHz was applied between the coil electrode inside the balloon and the 4 cutaneous electrode patches on the patient's back, thereby inducing capacitive-type heating of the balloon. The central balloon temperature was maintained at the target value (70°C or 73°C) by delivering vibratory waves through the lumen into the balloon to agitate the fluid inside. RF-generated thermal energy was applied to the RSPV antrum for 210 seconds, to the RIPV antrum

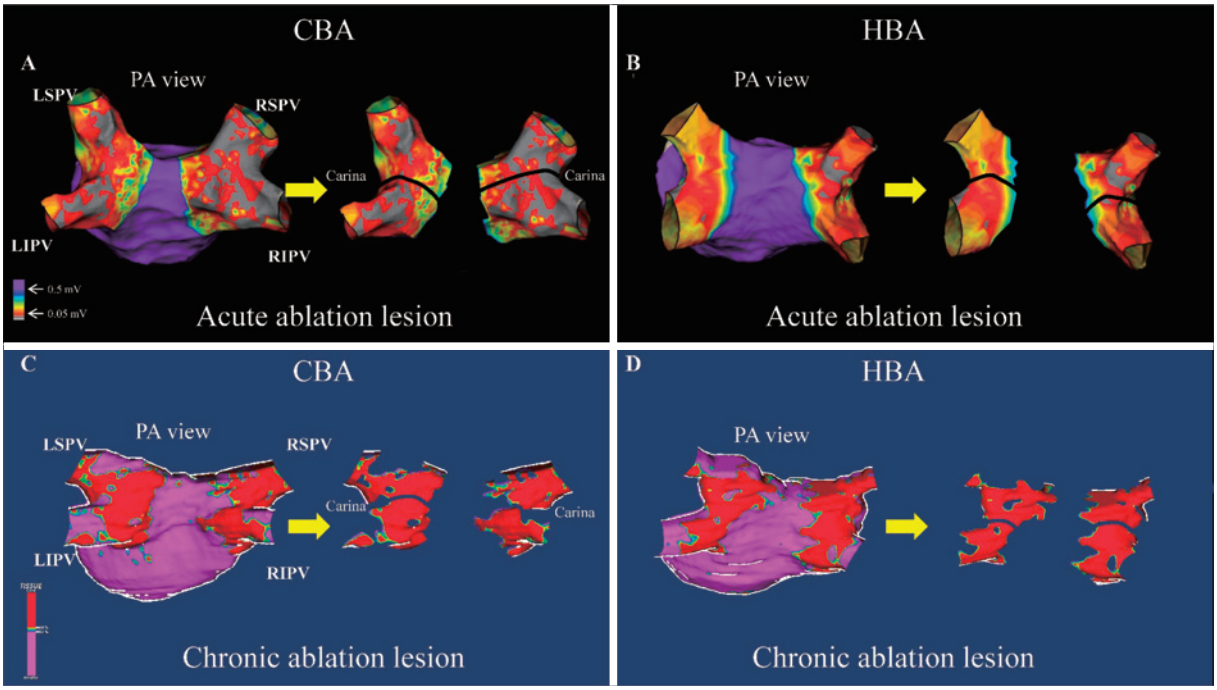

Fig. 1 Representative examples of post-ablation 3D voltage maps (left panels) and segmented ablation lesions (right panels) in the CBA and HBA groups (A and B) and chronic cMRI images and segmented ablation lesions (right panels) in the CBA and HBA groups (C and D). The 3D cMRI images display purple for healthy tissue, red for dense fibrotic tissue, and blue to yellow for intermediate fibrotic tissue (C and D). The total acute ablation lesion area and %acute ablation lesion area are larger for CBA than for HBA (55.2 cm^2 vs. 40.8 cm^2 and 32.4% vs. 22.0%, respectively), but the difference in ablation lesion area was less in the chronic cMRI images (36.2 cm^2 vs. 28.2 cm^2 and 24.6% and 21.7%, respectively). The details are shown in the text.
cMRI, cardiac magnetic resonance image; CBA, cryoballoon ablation; D, dimensional; HBA, hot balloon ablation; PV, pulmonary vein; LS, left superior PV; LI, left inferior; RS, right superior; RI, right inferior; PA view, posterior-anterior view.

and LIPV antrum for 150 seconds, and to the LSPV antrum for 240 seconds (70°C) or 180 seconds (73°C). To avoid esophageal injury, when the esophageal temperature exceeded 39°C, cooling saline was injected into the esophagus via a nasoesophageal tube. In both balloon technologies, phrenic nerve pacing was performed, and compound motor action potentials were recorded and monitored to detect phrenic nerve injury during application of thermal energy to the RSPV and RIPV[6].

Residual PV potentials were defined as residual electrical signals at the PV-LA junction assessed by the mapping catheter immediately after a single shot of CBA or HBA. Spontaneous PV reconnections were defined as spontaneous PV reconnections on a post-3D voltage map, 30 minutes after PVI was confirmed by single-shot CBA or HBA. If spontaneous PV reconnections and residual PV potentials were noted, additional touch-up RF ablation was performed at those sites with a 4-mm-tip catheter (Flexibility, Abbott or TactiCath, Abbott) to achieve PVI. Thereafter, a bolus of ATP 30 mg was injected to unmask any dormant PV conduction (DC). If ATP-provoked DC was identified by a mapping catheter, additional touch-up RF ablation was performed until no DC was provoked by a repeat ATP injection.

cMRI Acquisition and 3D Image Processing

cMRI was performed 3 months after ablation. The acquisition protocol has been previously reported[13]. In brief, images were acquired 15 min after an intravenous bolus injection of gadobutrol 0.2 mmol/kg (Gadvist, Bayer, Osaka, Japan) by a 1.5T scanner (Achieva 1.5T, Philips, The Netherland), using an ECG-gated sequence with a respiratory navigator. The voxel size was 1.4 mm × 1.4 mm × 1.4 mm.

Post-3D image processing of cMRI data was performed with ADAS-AF software (Galgo Medical, Barcelona, Spain), as described previously[13,19]. LA myocardium delineation was performed by manually drawing the midwall of the LA in each axial, sagittal, and coronal cMRI slice plane and automatically interpolating the delineation with software. The software then generated a 3D model of the LA from the slice-by-slice segmentation. The ADAS-AF software could evaluate fibrosis of the LA

wall and calculate LA volume and surface area. Values for healthy or dense scar tissue were validated previously. In brief, the image intensity ratio (IIR) was calculated as the ratio of the voxel intensity of the LA myocardium to the average intensity of the LA blood pool. An IIR ≤1.20 indicates healthy tissue, an IIR between >1.20 and ≤1.32 indicates interstitial fibrosis, and an IIR ≥1.32 is classified as dense fibrotic tissue[19]. The 3D model displayed purple for healthy tissue, red for dense fibrotic tissue, and blue to yellow for intermediate fibrotic tissue (**Fig. 1C, D**). An LA wall with an IIR ≥1.32 localized around the PV was defined as the total chronic ablation lesion area (cm^2). In principle, the measurements were identical to those for the acute ablation lesions, as described above. The %chronic ablation lesion area was calculated as the total chronic ablation lesion area (cm^2) (or chronic ablation lesion area in each PV)/ total PV-LA surface area (cm^2).

Post-Ablation Follow-Up

All AADs were resumed after ablation but then typically stopped after a 3-month blanking period. In some patients, AADs were continued beyond this point, in accordance with the preference of the physician and/or patient, even in the absence of AF recurrence. All patients underwent a routine follow-up examination at our outpatient clinic at 2 weeks and 1 month after ablation and at 1- to 3-month intervals thereafter for at least 6 months; 24-hour Holter monitoring was performed at 3 to 6 and 12 months after ablation. An electrocardiographic event recorder was used if patients reported any cardiac symptom. Any AF episode persisting longer than 30 seconds and documented on a standard electrocardiogram, event recorder, or 24-hour Holter monitor was considered an AF recurrence.

Statistical Analysis

Propensity scores for the treatment strategy (CBA or HBA) were obtained by logistic regression analysis of each of the 80 patients. The matching variables included sex, age, body mass index, AF subtype, congestive heart failure, hypertension, diabetes, stroke/transient ischemic attack, ejection fraction, and left atrial diameter. Matching was done without replacement and was based on logit-transformed propensity scores matched to the nearest neighbor in a 1:1 fashion with a caliper of 0.05. Continuous variables are expressed as means ± SD or medians with interquartile ranges. Differences in continuous variables between the 2 groups were analyzed with the Student t test or Mann-Whitney U test, as appropriate. The chi-square test was used to analyze differences in dichotomous variables, unless the expected values in the cells were <5, in which case the Fisher exact test was used. The paired t test was used to compare acute and chronic ablation lesions. Kaplan-Meier curves were drawn for freedom from AF recurrence, and differences between the 2 ablation groups were analyzed with the log-rank test. All statistical analyses were performed with JMP 11.2.0 software (SAS Institute, Cary, NC, USA). A p value of <0.05 was accepted as statistically significant.

Results

Patient Characteristics

The patient characteristics and echocardiographic variables in each study group are shown in **Table 1**. Because of propensity score matching, patient characteristics and echocardiographic findings were well-balanced between the HBA and CBA groups. The duration of cMRI acquisition from ablation was similar in the CBA and HBA groups. Analysis of anatomical cMRI-LA images showed no difference between the CBA and HBA groups in median LA volume or surface area on MRI scans. Total ablation procedure time was significantly shorter in the CBA group than in the HBA group (130±42 minutes vs. 155±38 minutes, $p = 0.03$) (**Table 1**).

Acute Ablation Lesion Area Assessed by Voltage Mapping and cMRI-Derived Chronic Ablation Lesion Area after CBA and HBA

Representative acute and chronic ablation lesions by CBA and HBA are shown in **Figure 1**. On the voltage map, the total acute ablation lesion area was larger in the CBA group than in the HBA group (54.9±12.0 cm^2 vs. 34.6±8.4 cm^2, $p < 0.001$). The %acute ablation lesion area was also larger in the CBA group than in the HBA group (30.8±5.8% vs. 23.0±5.5%, $p < 0.001$). The acute ablation lesion area in all PVs was larger in the CBA group than in the HBA group, and the tendency was similar for %acute ablation lesion area (**Table 2**). There was no difference between the CBA and HBA groups in total chronic ablation lesion area derived by cMRI (34.1±15.6 cm^2 vs. 29.4±15.9 cm^2, $p = 0.31$). The %chronic ablation lesion area did not differ between the 2 groups (24.8±10.8% vs. 21.1±11.6%, $p = 0.26$). Chronic ablation lesion area and %chronic ablation lesion area did not differ between the 2 groups for any PV (**Table 2**).

Difference in %acute Ablation Lesion Area Assessed by Voltage Mapping and cMRI-Derived %chronic Ablation Lesion Area

In the CBA group, %acute ablation lesion area decreased significantly in the chronic phase, from 30.8±5.8%

Table 1 Patient characteristics and echocardiographic and cMRI parameters, by study group

	CBA (n=24)	HBA (n=24)	*p* Value
Age (years)	63±10	62±9	0.66
Male sex	17 (71)	17 (71)	1.00
Body mass index (kg/m^2)	25±5	24±3	0.45
Paroxysmal AF	17 (71)	17 (71)	1.00
Comorbidities			
Heart failure	1 (2)	1 (2)	1.00
Hypertension	16 (67)	12 (50)	0.24
Diabetes	4 (8)	4 (8)	1.00
History of stroke	0 (0)	1 (4)	1.00
Vascular disease	0 (0)	1 (4)	1.00
CHA_2DS_2-VASc score	1 (1-3)	1 (1-2)	1.00
Echocardiographic parameters			
Ejection fraction (%)	68±11	66±7	0.66
LA diameter (mm)	39±5	39±6	0.87
LA volume (mL)	45±16	43±19	0.70
cMRI parameters			
cMRI acquisition during ablation (months)	3 (3-4)	3 (3-4)	0.96
LA volume (mL)	84.4±23.6	92.9±23.9	0.22
LA surface area (cm^2)	135.8±17.1	139.5±17.4	0.45
Gap numbers per patient	3 (2-5)	3 (1-9)	0.24
Ablation procedure time (minutes)	130±42	155±38	0.03
Antiarrhythmic drugs used after ablation	11 (46)	10 (42)	0.77
Class I	2 (8)	1 (4)	0.55
Class III (amiodarone)	1 (4)	0 (0)	0.14
Class IV (bepridil)	8 (33)	9 (38)	0.76

Values are shown as mean±SD, median (interquartile range), or number (%).
AF, atrial fibrillation; CBA, cryoballoon ablation; CHA_2DS_2-VASc, congestive heart failure=1, hypertension=1, age ≥75 years=2, diabetes=1, stroke/TIA=2, vascular disease=1, age 65–74 years=1, and female sex=1; cMRI, cardiac magnetic resonance image; HBA, hot balloon ablation; LA, left atrial.

to 24.8±10.8% (p = 0.038); this decrease was pronounced for the LSPV (p = 0.026) and RIPV (p = 0.001) (**Fig. 2A**). There was no significant difference between %acute ablation lesion area and %chronic ablation lesion area in the HBA group (p = 0.46), but the decrease for the LSPV was significant (**Fig. 2B**). Nadir CBA balloon temperature positively correlated with Δ%ablation lesion area (calculated as %acute ablation lesion area minus %chronic ablation lesion area) (r = 0.22, p = 0.030), and this correlation was greater for the LSPV and RIPV (r = 0.35, p = 0.016) (**Fig. 3**).

Touch-Up Ablation for Acute PV Reconnections after CBA and HBA

PVI was achieved in all patients. Touch-up RF ablation was less frequently necessary in the CBA group—including 2/24 (8%) patients with 9 (2%) of 480 (20 segments × 24 patients) segments—than in the HBA group—including 14/24 (58%) patients with 36/480 (8%) segments (p < 0.001 per patient and segment). Touch-up RF ablation was often required at the inferior segment of the RIPV in the CBA group (3/9 [33%] segments) and at the carina-anterior segment of the LSPV in the HBA group (8/36 [22%] segments).

Complications

Pericardial tamponade occurred in 1 patient in the HBA group; no complications occurred in the CBA group. There were no periprocedural deaths in either group.

Post-Ablation Treatment and Ablation Outcomes

After the ablation procedure, 11 patients (46%) in the CBA group and 10 patients (42%; p = 0.77) in the HBA group were given AADs to maintain SR. There were no between-group differences in the number of patients given a class I drug (2 [8%] vs. 1 [4%], respectively; p = 0.55), class III drug (amiodarone) (1 [4%] vs. 0 [0%], respectively; p = 0.14), or class IV drug (bepridil) (8 [33%]

Table 2 Acute ablation lesion area and %ablation lesion, as assessed by voltage mapping, and cMRI-derived chronic ablation lesion size in the CBA and HBA groups

	CBA (n=24)	HBA (n=24)	*p* value
Acute ablation lesion area, cm²	54.9±12.0	34.6±8.4	<0.001
LSPV	12.2±3.9	7.7±2.2	<0.001
LIPV	13.0±5.3	7.5±2.8	<0.001
RSPV	15.3±6.2	10.6±3.4	0.003
RIPV	15.0±4.1	8.8±3.8	<0.001
%acute ablation lesion, %	30.8±5.8	23.0±5.5	<0.001
LSPV	6.8±2.0	5.1±2.5	0.002
LIPV	7.1±2.0	5.0±1.9	0.001
RSPV	8.6±3.4	7.1±2.3	0.08
RIPV	8.6±2.7	5.9±2.5	0.001
Chronic ablation lesion area, cm²	34.1±15.6	29.4±15.9	0.31
LSPV	7.1±4.8	5.6±3.7	0.21
LIPV	8.9±6.5	7.3±4.5	0.32
RSPV	11.4±4.9	10.6±5.7	0.61
RIPV	7.5±4.0	7.2±5.6	0.84
%chronic ablation lesion, %	24.8±10.8	21.2±11.6	0.26
LSPV	5.2±3.3	4.1±2.8	0.20
LIPV	6.6±4.6	5.2±3.0	0.22
RSPV	8.3±3.1	7.7±4.3	0.59
RIPV	5.5±2.9	5.2±4.2	0.79

Values are shown as mean±SD.
cMRI, cardiac magnetic resonance image; CBA, cryoballoon ablation; HBA, hot balloon ablation; LS, left superior; LI, left inferior; RS, right superior; RI, right inferior; PV, pulmonary vein.

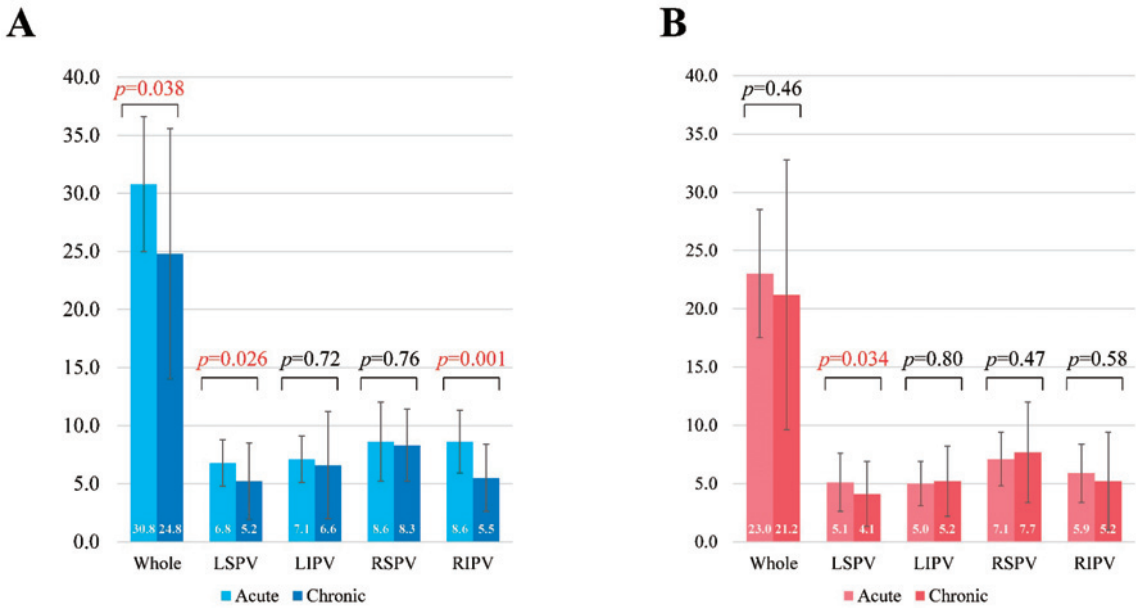

Fig. 2 Difference in %acute ablation lesion area and %chronic ablation lesion area after CBA (A) and HBA (B).
CBA, cryoballoon ablation; HBA, hot balloon ablation; PV, pulmonary vein; LS, left superior PV; LI, left inferior; RS, right superior; RI, right inferior.

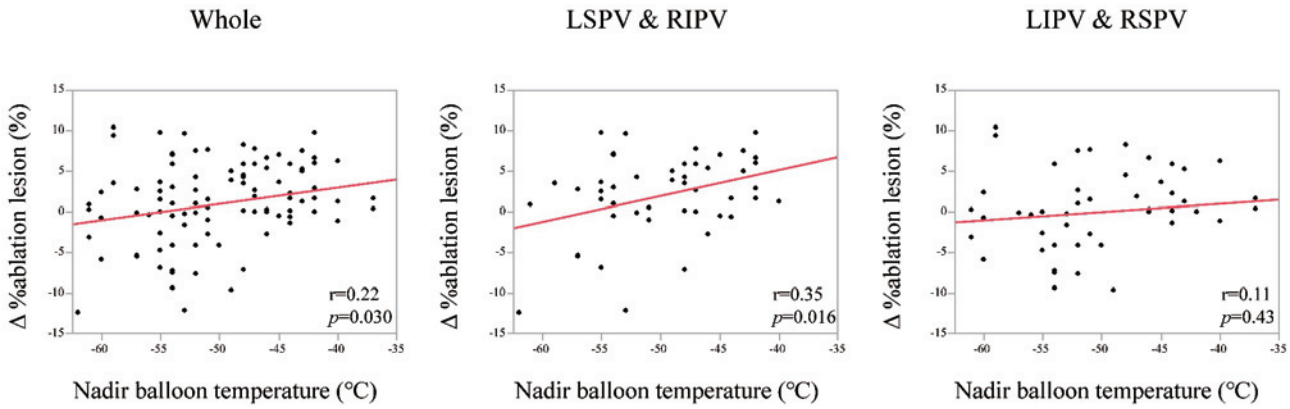

Fig. 3 Correlation of nadir balloon temperature during CBA with Δ%ablation lesions from %acute ablation lesion area minus %chronic ablation lesion area. PV, pulmonary vein; LS, left superior PV; LI, left inferior; RS, right superior; RI, right inferior.

vs. 9 [38%], respectively; p = 0.76, **Table 1**). During a median of 17.6 (12.6-25.3) months, the rate of AF recurrence did not significantly differ between the CBA and HBA groups (12.5% vs. 8.3%, p = 0.45 by log-rank test). cMRI-derived LA volume and surface area were significantly greater in patients with AF recurrence than in those without AF recurrence (LA volume: 109.9±4.6 mL vs. 86.2±24.0 mL, p = 0.033; LA surface area: 153.8±9.0 cm^2 vs. 135.8±16.9 cm^2, p = 0.024). There was no difference in the other variables, including the patient characteristics and echocardiographic parameters shown in **Table 1**, and %chronic ablation lesion area (27±8% vs. 23±12%, p = 0.39), between those with and without chronic AF recurrence.

Discussion

The main findings of this study were as follows: 1) cMRI-derived chronic ablation lesion area was quantitatively equivalent in the CBA and HBA groups, but acute ablation lesion area, as assessed by voltage mapping, was significantly larger in the CBA group, 2) there was no significant difference in the rate of AF recurrence after CBA and HBA, and 3) LA volume and LA surface area were strongly associated with AF recurrence, but %ablation lesion area was not.

Comparison of Ablation Lesions after CBA and HBA

In 3D voltage maps, the acute ablation lesion area was significantly larger after CBA than after HBA, which is consistent with a previous study. That study explained that the larger acute ablation lesions after CBA may result from the larger balloon surface-tissue contact area, where the more proximal portion of the PV antrum is distorted by the stiff CBA, while HBA is highly compliant with the PV antrum surface, because of the narrower balloon surface-tissue contact area at a more distal portion of the PV antrum[4]. However, the present study showed no difference in chronic ablation lesion area between the 2 balloon ablation modalities. A study using atrial late gadolinium enhancement-MRI analysis reported that atrial scarring was correlated with colocalized low-voltage measurements in the same phase[20]. Therefore, 3D voltage map-based acute ablation lesion area after CBA would be lower during the chronic phase if the 3D-voltage map was obtained during the chronic phase. Furthermore, Yamashita et al. reported the presence of acute edema immediately after cryoablation, which resolved within 1 to 2 weeks[21]. Acute ablation lesions after CBA significantly regressed during the chronic phase on high-resolution voltage mapping[22]. Past and present evidence suggests that, because of insufficient energy penetration and/or acute edema, the ablation lesion area may have been overestimated when compared with subsequent chronic ablation lesions assessed by cMRI imaging.

However, the lack of change in acute and chronic ablation lesion areas in the HBA group may be attributable to the differences in energy characteristics. The cooling convective thermal energy of CBA is a milder, safer energy source than the heating convective thermal energy of radiofrequency sources. Therefore, once convective thermal energy-dependent HBA creates ablation lesions with good balloon surface contact, acute ablation lesions may be irreversible and persistent; thus, later decreases may be small. Taken together, the present findings provide mechanistic insights into differences in lesion formation between CBA and HBA.

Chronic Lesions and Clinical Outcome

After CBA and HBA, the decrease from %acute abla-

tion lesion area to %chronic ablation lesion area was pronounced for the LSPV. Miyazaki et al. reported that recurrent AF originating from the LSPV antrum could not be isolated by the CBA[23]. In the present study, the touch-up RF ablation site was often at the inferior segment of the RIPV in the CBA group and at the carina-anterior segment of the LSPV in the HBA group, as has been reported previously[6,10]. In patients with recurrence after CBA, PV reconnections were associated with recurrence in approximately 30% of patients, 87% of whom had reconnections of at least an upper PV. Therefore, although PV reconnection sites were not evaluated in this study, chronic PV reconnection sites associated with AF recurrence (i.e., the LSPV and/or LSPV carina region) might be similar for CBA and HBA. This hypothesis is partially supported by our finding of no difference in chronic lesion size between the 2 groups. Thus, as was the case in previous studies[4,6], we observed a low rate of AF recurrence and no significant difference between the CBA and HBA groups in this small study ($p = 0.45$). A higher nadir CBA balloon temperature was strongly associated with a decrease in Δ%ablation lesion area, in particular for the LSPV and RIPV ($r = 0.35$, $p = 0.016$). This suggests that greater regression in CBA lesions during the chronic phase may depend in part on higher nadir CBA balloon temperature, because of insufficient CB-tissue surface contact. When the nadir CBA balloon temperature is inadequate, the patient should be monitored for any spontaneous PV conduction, residual PV potentials, or ATP-provoked DC after CBA, to prevent chronic regression of CBA. Yamasaki et al. demonstrated the importance of maintaining coaxial position when performing HBA procedures[24]. Therefore, upper PV PVI durability can likely be improved by maintaining good balloon surface-tissue contact, and bonus ablation to the PV antra might improve outcomes after CBA and HBA[25].

Limitations

Our study had several limitations. First, it was limited by the size of the patient groups. However, after propensity matching, the patients in the 2 groups were well-balanced, so any bias from patient background was minimized. Second, we could not perform voltage mapping during the chronic phase; thus, it remains unclear whether our cMRI scans directly reflected voltage maps in the chronic phase. However, voltage map creation in the chronic phase presents ethical concerns, especially in patients without AF recurrence. To minimize the effect of differences in assessment method, we investigated chronological changes in %ablation lesion area by calculating relative ablation lesion area to total PV-LA surface area. In addition, the decrease from an acute lesion of CBA to a chronic lesion identified by high-resolution voltage mapping, as reported previously[22], at least supported our finding identified in CBA lesions. Third, acute PV reconnection sites were not assessed by cMRI in the chronic phase because we performed additional ablation of PV reconnection sites.

Conclusions

Acute ablation lesions assessed by voltage mapping appeared to be significantly larger after CBA than after HBA, but CBA lesions may decrease in size during the chronic phase, thereby resulting in similar chronic ablation lesion areas after CBA and HBA.

Author contributions: Concept/design: R.W., Y.O. and K.N.
Data analysis/interpretation: R.W., Y.O., and K.N.
Drafting article: R.W. and Y.O.
Critical revision of the article: R.W., Y.O., K.N., Y.W., A. Y., S.K.
Approval of the article: R.W., Y.O., K.N., Y.W., A.Y., S. K.
Statistics: R.W. and Y.O.
Data collection: R.W., Y.W. and N.O.

Acknowledgements: We thank Mr. Martin John for his help in preparing this article.

Conflict of Interest: The study was supported by departmental resources only, and the authors have no conflict of interest to declare.

References

1. Giovanni GD, Wauters K, Chierchia GB, et al. One-year follow-up after single procedure Cryoballoon ablation: a comparison between the first and second generation balloon. J Cardiovasc Electrophysiol [Internet]. 2014 Aug;25 (8):834–9. Available from: https://onlinelibrary.wiley.com/doi/pdfdirect/10.1111/jce.12409?download=true
2. Fürnkranz A, Bordignon S, Dugo D, et al. Improved 1-year clinical success rate of pulmonary vein isolation with the second-generation cryoballoon in patients with paroxysmal atrial fibrillation. J Cardiovasc Electrophysiol [Internet]. 2014 Aug;25(8):840–4. Available from: https://onlinelibrary.wiley.com/doi/pdfdirect/10.1111/jce.12417?download=true
3. Chierchia GB, Di Giovanni G, Ciconte G, et al. Second-generation cryoballoon ablation for paroxysmal atrial fibrillation: 1-year follow-up. Europace [Internet]. 2014 May; 16(5):639–44. Available from: https://academic.oup.com/europace/article/16/5/639/484579?login=true
4. Nagashima K, Okumura Y, Watanabe I, et al. Hot balloon versus cryoballoon ablation for atrial fibrillation: Lesion

characteristics and middle-term outcomes. Circ Arrhythm Electrophysiol [Internet]. 2018 May;11(5):e005861. Available from: https://www.ahajournals.org/doi/pdf/10.1161/CIRCEP.117.005861?download=true
5. Sohara H, Ohe T, Okumura K, et al. Hotballoon ablation of the pulmonary veins for paroxysmal AF: A multicenter randomized trial in Japan. J Am Coll Cardiol [Internet]. 2016 Dec 27;68(25):2747–57. Available from: https://www.sciencedirect.com/science/article/pii/S073510971636819X?via%3Dihub
6. Wakamatsu Y, Nagashima K, Nakahara S, et al. Electrophysiologic and anatomic factors predictive of a need for touch-up radiofrequency application for complete pulmonary vein isolation: Comparison between hot balloon- and cryoballoon-based ablation. J Cardiovasc Electrophysiol [Internet]. 2019 Aug;30(8):1261–9. Available from: https://onlinelibrary.wiley.com/doi/pdfdirect/10.1111/jce.13989?download=true
7. Stabile G, Di Donna P, Schillaci V, et al. Safety and efficacy of pulmonary vein isolation using a surround flow catheter with contact force measurement capabilities: A multicenter registry. J Cardiovasc Electrophysiol [Internet]. 2017 Jul;28(7):762–7. Available from: https://onlinelibrary.wiley.com/doi/pdfdirect/10.1111/jce.13227?download=true
8. De Potter T, Van Herendael H, Balasubramaniam R, et al. Safety and long-term effectiveness of paroxysmal atrial fibrillation ablation with a contact force-sensing catheter: real-world experience from a prospective, multicentre observational cohort registry. Europace [Internet]. 2018 Nov 1;20(Fi_3):f410–8. Available from: https://academic.oup.com/europace/article/20/FI_3/f410/4791150?login=true
9. Okumura Y, Watanabe I, Iso K, et al. Mechanistic insights into durable pulmonary vein isolation achieved by second-generation cryoballoon ablation. J Atr Fibrillation [Internet]. 2017 Apr-May;9(6):1538. Available from: https://www.ncbi.nlm.nih.gov/pmc/articles/PMC5673339/pdf/jafib-09-01538.pdf
10. Watanabe R, Okumura Y, Nagashima K, et al. Influence of balloon temperature and time to pulmonary vein isolation on acute pulmonary vein reconnection and clinical outcomes after cryoballoon ablation of atrial fibrillation. J Arrhythm [Internet]. 2018 Oct;34(5):511–9. Available from: https://www.ncbi.nlm.nih.gov/pmc/articles/PMC6174370/pdf/JOA3-34-511.pdf
11. Inamura Y, Nitta J, Inaba O, et al. Differences in the electrophysiological findings of repeat ablation between patients who first underwent cryoballoon ablation and radiofrequency catheter ablation for paroxysmal atrial fibrillation. J Cardiovasc Electrophysiol [Internet]. 2019 Oct;30(10):1792–800. Available from: https://onlinelibrary.wiley.com/doi/pdfdirect/10.1111/jce.14065?download=true
12. Glowniak A, Tarkowski A, Fic P, Wojewoda K, Wojcik J, Wysokinski A. Second-generation cryoballoon ablation for recurrent atrial fibrillation after an index procedure with radiofrequency versus cryo: Different pulmonary vein reconnection patterns but similar long-term outcome-Results of a multicenter analysis. J Cardiovasc Electrophysiol [Internet]. 2019 Jul;30(7):1005–12. Available from: https://onlinelibrary.wiley.com/doi/pdfdirect/10.1111/jce.13938?download=true
13. Figueras IVRM, M ă rgulescu AD, Benito EM, et al. Post-procedural LGE-CMR comparison of laser and radiofrequency ablation lesions after pulmonary vein isolation. J Cardiovasc Electrophysiol [Internet]. 2018 Aug;29(8):1065–72. Available from: https://onlinelibrary.wiley.com/doi/pdfdirect/10.1111/jce.13616?download=true
14. Kurose J, Kiuchi K, Fukuzawa K, et al. The lesion characteristics assessed by LGE-MRI after the cryoballoon ablation and conventional radiofrequency ablation. J Arrhythm [Internet]. 2018 Apr;34(2):158–66. Available from: https://www.ncbi.nlm.nih.gov/pmc/articles/PMC5891401/pdf/JOA3-34-158.pdf
15. Khurram IM, Catanzaro JN, Zimmerman S, et al. MRI evaluation of radiofrequency, cryothermal, and laser left atrial lesion formation in patients with atrial fibrillation. Pacing Clin Electrophysiol [Internet]. 2015 Nov;38(11):1317–24. Available from: https://onlinelibrary.wiley.com/doi/pdfdirect/10.1111/pace.12696?download=true
16. Cochet H, Mouries A, Nivet H, et al. Age, atrial fibrillation, and structural heart disease are the main determinants of left atrial fibrosis detected by delayed-enhanced magnetic resonance imaging in a general cardiology population. J Cardiovasc Electrophysiol [Internet]. 2015 May;26(5):484–92. Available from: https://onlinelibrary.wiley.com/doi/pdfdirect/10.1111/jce.12651?download=true
17. Marrouche NF, Wilber D, Hindricks G, et al. Association of atrial tissue fibrosis identified by delayed enhancement MRI and atrial fibrillation catheter ablation: the DECAAF study. JAMA [Internet]. 2014 Feb 5;311(5):498–506. Available from: http://diposit.ub.edu/dspace/bitstream/2445/119599/1/658277.pdf
18. Platonov PG, Mitrofanova LB, Orshanskaya V, Ho SY. Structural abnormalities in atrial walls are associated with presence and persistency of atrial fibrillation but not with age. J Am Coll Cardiol [Internet]. 2011 Nov 15;58(21):2225–32. Available from: https://www.sciencedirect.com/science/article/pii/S0735109711030804?via%3Dihub
19. Benito EM, Carlosena-Remirez A, Guasch E, et al. Left atrial fibrosis quantification by late gadolinium-enhanced magnetic resonance: a new method to standardize the thresholds for reproducibility. Europace [Internet]. 2017 Aug 1;19(8):1272–9. Available from: http://diposit.ub.edu/dspace/bitstream/2445/116243/1/664770.pdf
20. Malcolme-Lawes LC, Juli C, Karim R, et al. Automated analysis of atrial late gadolinium enhancement imaging that correlates with endocardial voltage and clinical outcomes: a 2-center study. Heart Rhythm [Internet]. 2013 Aug;10(8):1184–91. Available from: https://www.sciencedirect.com/science/article/pii/S1547527113005080?via%3Dihub
21. Yamashita K, Kholmovski E, Ghafoori E, et al. Characterization of edema after cryo and radiofrequency ablations based on serial magnetic resonance imaging. J Cardiovasc Electrophysiol [Internet]. 2019 Feb;30(2):255–62. Available from: https://onlinelibrary.wiley.com/doi/pdfdirect/10.1111/jce.13785?download=true
22. Sekihara T, Miyazaki S, Aoyama D, et al. Evaluation of cryoballoon pulmonary vein isolation lesions during the acute and chronic phases using a high-resolution mapping system. J Interv Card Electrophysiol [Internet]. 2022 Apr 30. Available from: https://link.springer.com/content/pdf/10.1007/s10840-022-01225-w.pdf
23. Miyazaki S, Taniguchi H, Hachiya H, et al. Quantitative analysis of the isolation area during the chronic phase after a 28-mm second-generation cryoballoon ablation demarcated by high-resolution electroanatomic mapping. Circ Arrhythm Electrophysiol [Internet]. 2016 May;9(5):e003879. Available from: https://www.ahajournals.org/doi/pdf/10.1161/CIRCEP.115.003879?download=true
24. Yamasaki H, Aonuma K, Shinoda Y, et al. Initial result of antrum pulmonary vein isolation using the radiofre-

quency hot-balloon catheter with single-shot technique. JACC Clin Electrophysiol [Internet]. 2019 Mar;5(3):354–63. Available from: https://www.sciencedirect.com/science/article/pii/S2405500X19300714?via%3Dihub
25. Miyazaki S, Horie T, Hachiya H, et al. The mechanisms of recurrent atrial arrhythmias after second-generation cryoballoon ablation. Am Heart J [Internet]. 2020 Mar;221:29–38. Available from: https://www.sciencedirect.com/science/article/pii/S0002870319303424?via%3Dihub

(Received, July 8, 2022)
(Accepted, August 24, 2022)
(J-STAGE Advance Publication, November 25, 2022)